JOURNAL OF GUIDANCE, CONTROL, AND DYNAMICS
Vol. 25, No. 3, May–June 2002

Minimizing the Effects of Transverse Torques During Thrusting for Spin-Stabilized Spacecraft

James A. Oldenburg* and Steven G. Tragesser†
Air Force Institute of Technology, Wright–Patterson Air Force Base, Ohio 45433

During an orbital maneuver of a spin-stabilized spacecraft, undesired transverse torques are present due to thruster misalignment and offset from the center of mass. These body-fixed torques cause the thrust vector to precess about a direction that is offset from the nominal. This oscillation of the thrust vector over the course of the maneuver decreases the final magnitude of the ΔV while the average offset causes a pointing error. Previous work shows that inserting a short-coast phase into the maneuver can eliminate the pointing error. The behavior of the thrust axis is considered to find solutions for the coast phase timing that minimize the average oscillation of the thrust axis to maximize ΔV, while retaining the property of eliminating the secular pointing error. The new maneuver scheme realizes a significant increase in efficiency over the previous solution, particularly if the oscillation of the thrust axis is large.

I. Introduction

SPIN stabilization is a common method of maintaining a desired orientation in the presence of disturbing torques. This technique can be used, for example, for a spacecraft and inertial upper stage before an orbital insertion maneuver from a low Earth parking orbit to a geostationary orbit. Because of manufacturing errors and uncertainties, however, the force from the spacecraft thruster or inertial upper stage will not be perfectly aligned with the spacecraft center of mass as shown to an exaggerated degree in Fig. 1.

The thruster offset or misalignment results in a constant body-fixed moment, which in turn causes the spin/thrust axis of the spacecraft to precess as shown in the left diagram of Fig. 2a. The middle diagram of Fig. 2a shows the incremental ΔV for small time spans as the satellite is thrusting and spinning. (Note that the thrust axis precession is more complicated than the circular path depicted in this simplified illustration.) If the thruster is perfectly aligned, the case is nominal with no precession, and the incremental ΔV are colinear along the desired direction. With a small transverse torque, however, the incremental ΔV are along the precessing thrust axis, which is generally not in the desired direction. The right diagram in Fig. 2a shows the summation of the incremental ΔV. The final ΔV for the precessing satellite is smaller in magnitude than the nominal ΔV and not aligned in the nominal direction. Thus, the misaligned or offset thruster has the undesirable effect of both decreasing the magnitude of the total ΔV and causing a pointing error.

In Ref. 1 a method of momentarily disrupting the thrust is described that causes the thrust axis precession to be centered about its initial (desired) direction as shown in Fig. 2b. This two-burn scheme eliminates the pointing error, but may have a significant loss in the total ΔV because the thrust axis still deviates from the desired direction. Reference 1 and subsequent work[2,3] focus on eliminating the pointing error, but do not attempt to maximize the final ΔV. The improved two-burn scheme developed here also uses a momentary disruption of thrust to eliminate the velocity pointing errors. In addition, the burn and coast times are selected to minimize the deviation of the thrust axis from the desired ΔV direction as shown in Fig. 2c. This approach maximizes the magnitude of the final ΔV.

II. Two-Burn Scheme

The two-burn scheme was developed by Longuski et al.[1] to reduce pointing errors for thrusting, axisymmetric, spin-stabilized spacecraft. The theory was developed by analyzing the behavior of the angular momentum vector. The authors assume that the spacecraft is initially spinning perfectly along the desired direction of the ΔV, which is aligned with the inertial Z axis in Fig. 3. When the thruster is ignited, a thruster offset causes a transverse torque M_x, which is assumed to be about the body x axis without loss of generality. It is shown in Ref. 1 that, for a small transverse torque, the inertial components of the angular momentum vector are

$$H_X = (M_x/\Omega)\sin\Omega t, \qquad H_Y = (M_x/\Omega)(1-\cos\Omega t)$$
$$H_Z = I_z\Omega \tag{1}$$

where Ω is the inertial spin rate and I_z is the moment of inertia about the axis of symmetry, that is, the thrust axis. This behavior is shown in Fig. 3. The Z component is constant, whereas the X and Y components trace out a circle. This motion has an average bias ρ of

$$\rho = \tan^{-1}\left(M_x \big/ I_z\Omega^2\right) \approx M_x \big/ I_z\Omega^2 \tag{2}$$

In Ref. 1, the authors show that the secular pointing error of the velocity vector is equal to the ρ offset in the angular momentum. Thus, the behavior of the angular momentum vector appears to provide a good approximation for the behavior of the thrust axis. Based on this premise, Longuski et al. introduce a method to eliminate the pointing error in ΔV by centering the cone in Fig. 3 about the Z axis. The maneuver is shown in Fig. 4 in the inertial XY plane. After the angular momentum vector has rotated through 60 deg, the thrust is shut off (or otherwise disrupted). The spacecraft continues to spin, but the angular momentum vector is fixed in inertial space because there are no torques. If the spacecraft coasts for another 60-deg rotation about the thrust axis and then begins thrusting again, the new path of the angular momentum vector is centered about the Z axis, which is the desired direction of the ΔV. This eliminates the pointing error caused by the transverse torque. The duration of the initial burn, t_b, and the duration of the coast, t_c, are shown to be

$$t_b = t_c = \pi/3\Omega \tag{3}$$

This maneuver, firing the thruster for $\pi/3\Omega$ s and then coasting for $\pi/3\Omega$ s before resuming full thrust, constitutes the two-burn scheme from Ref. 1. Of course, waiting additional revolutions during either the burn or the coast phase also results in elimination of the pointing

Received 31 May 2001; revision received 20 September 2001; accepted for publication 6 November 2001.

*Graduate Student, Department of Aeronautics and Astronautics; currently Chief, National Missile Defense Command and Control Integration Section, U.S. Space Command, Peterson Air Force Base, Colorado 80914; james.oldenburg@peterson.af.mil.

†Assistant Professor, Department of Aeronautics and Astronautics; Steven.Tragesser@afit.edu. Member AIAA.

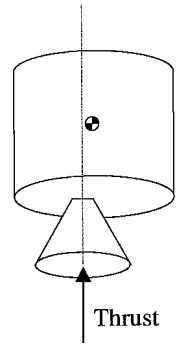

Fig. 1 Spacecraft thruster offset from center of mass.

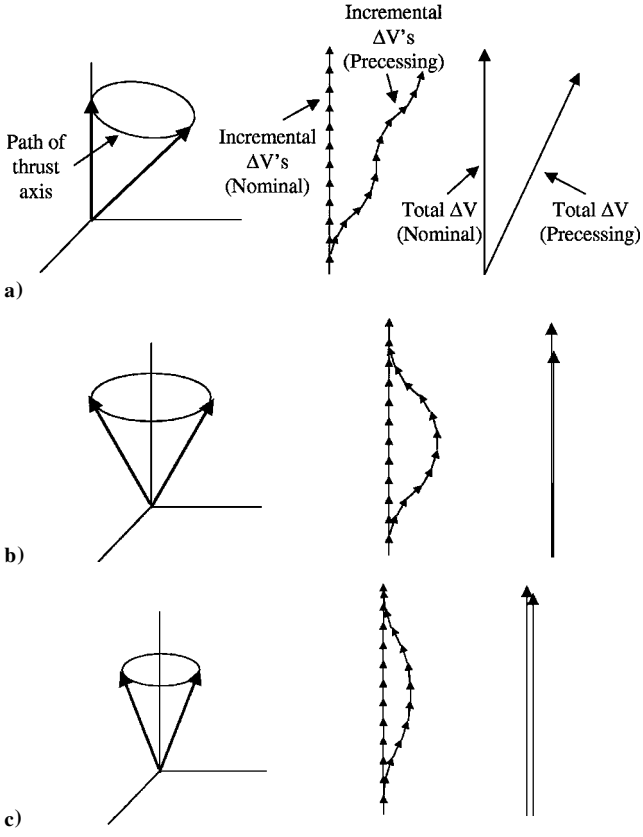

Fig. 2 Precession of thrust axis, incremental ΔV, and total ΔV for spin-stabilized spacecraft: a) constant thrust, ΔV pointing and magnitude errors; b) two-burn scheme, ΔV magnitude errors; and c) improved two-burn scheme, magnitude errors reduced.

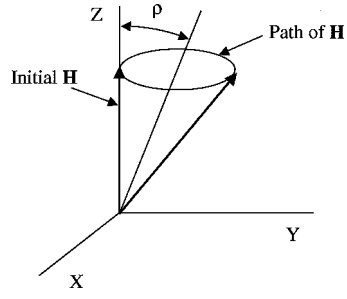

Fig. 3 Angular momentum vector during thrusting.

error. Thus, the full range of possible initial burn and coast times is

$$t_b = (\pi/3 + 2\pi m)/\Omega, \qquad t_c = (\pi/3 + 2\pi n)/\Omega \tag{4}$$

where m and n are each nonnegative integers pertaining to the number of additional revolutions during the initial burn and coast periods, respectively. On the basis of this angular momentum analysis, the maneuver is equivalent for each of the different possibilities of m and n. However, this conclusion does not hold when one considers the dynamics of the thrust axis.

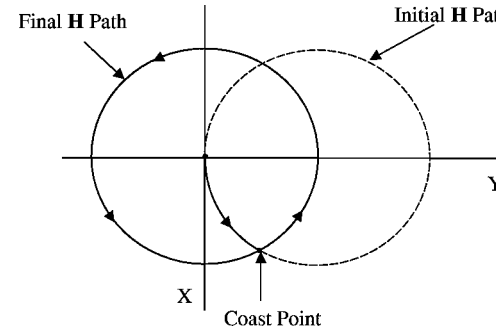

Fig. 4 Angular momentum vector for the two-burn scheme.

III. Improved Two-Burn Scheme

The approximate solution for the angular momentum used in the development of the two-burn scheme is very effective in eliminating pointing errors; however, the maneuver can be further improved on if we consider the dynamics of the spacecraft's thrust axis. As with the two-burn scheme, this maneuver has an initial burn time of t_b and then a coast time of t_c. As shown in Fig. 5, we use an Euler 1–2–3 sequence to describe the orientation of an axisymmetric spacecraft with respect to the inertial XYZ frame. Assuming that the deviations from the inertial Z axis are small, we can derive analytic expressions for the motion of the off-axis behavior of the axis of symmetry given by the θ_1 and θ_2 Euler angles about body x and y axes. (See "Results" section for the differential equations of motion.) After a duration t of the second burn, the solutions for the Euler angles are

$$\begin{aligned}\theta_1 &= (M_x/I_z\Omega\alpha)[-\cos(I_z\Omega t/I_x - \alpha t_b - \alpha t_c) + \cos(\Omega t_b + \Omega t_c) \\ &\quad + \cos(I_z\Omega t/I_x - \alpha t_b) - \cos(I_z\Omega t/I_x) - \cos(\Omega t_b)] \\ &\quad + (M_x/I_x\Omega\alpha)[\cos(\Omega t) - \cos(\Omega t_b + \Omega t_c) + \cos(\Omega t_b)] \\ &\quad - M_x \big/ I_z\Omega^2 \\ \theta_2 &= (M_x/I_z\Omega\alpha)[-\sin(I_z\Omega t/I_x - \alpha t_b - \alpha t_c) + \sin(\Omega t_b + \Omega t_c) \\ &\quad + \sin(I_z\Omega t/I_x - \alpha t_b) - \sin(I_z\Omega t/I_x) - \sin(\Omega t_b)] \\ &\quad + (M_x/I_x\Omega\alpha)[\sin(\Omega t) - \sin(\Omega t_b + \Omega t_c) + \sin(\Omega t_b)] \\ \theta_3 &= \Omega t\end{aligned} \tag{5}$$

where I_x and I_z are the moments of inertia perpendicular to and along the axis of symmetry, respectively. The parameter α is defined for convenience as

$$\alpha \equiv [(I_z - I_x)/I_x]\Omega \tag{6}$$

As in the two-burn case, we have assumed without loss of generality that the moment is about the x axis. This solution is similar to the one found by Wie[4] except this one has been formulated to include the coast phase and second burn.

Isolating the constant terms from Eqs. (5) yields the following offset of the thrust axis

$$\begin{aligned}\text{offset}_{\theta 1} &= \left(M_x \big/ I_z\Omega^2\right)[\cos(\Omega t_b + \Omega t_c) - \cos(\Omega t_b) + 1] \\ \text{offset}_{\theta 2} &= -\left(M_x \big/ I_z\Omega^2\right)[\sin(\Omega t_b + \Omega t_c) - \sin(\Omega t_b)]\end{aligned} \tag{7}$$

Setting the offset to zero, that is, eliminating pointing error, yields the same solutions for the burn and coast times given by Eqs. (4). That is, the solution for the burn and coast times to negate the pointing error is identical when considering either the angular momentum vector or the thrust axis. Unlike the angular momentum, however, the behavior of the thrust axis is not identical for different values of the integer revolutions m and n. Thus, the maneuver contains two additional degrees of freedom (m and n) that are not obvious with the approach from Ref. 1. The improved two-burn scheme uses these degrees of freedom to minimize the oscillation of the thrust axis (as in Fig. 2c).

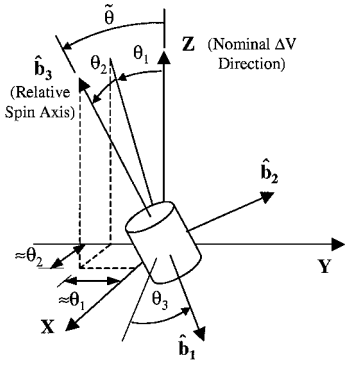

Fig. 5 Euler 1–2–3 angle sequence and angular offset $\tilde{\theta}$.

By inspection of the transformation matrix for the Euler 1–2–3 sequence, the angular deviation of the thrust axis away from the desired ΔV direction (Fig. 5) can be shown to be

$$\tilde{\theta} = \tan^{-1}\left(\frac{\sqrt{\cos^2\theta_1 \sin^2\theta_2 + \sin^2\theta_1}}{\cos\theta_1 \cos\theta_2}\right) \tag{8}$$

Assuming small angles yields

$$\tilde{\theta} \approx \sqrt{\theta_1^2 + \theta_2^2} \tag{9}$$

Therefore, the mean angular deviation from the desired ΔV direction is

$$\tilde{\theta}_{\text{avg}} = \frac{1}{t}\int_0^t \sqrt{\theta_1^2 + \theta_2^2}\,\mathrm{d}t = f(m, n) \tag{10}$$

where (for the improved two-burn scheme) we only need to substitute the time varying terms in θ_1 and θ_2 from Eqs. (5) into Eq. (10) because the constant terms in Eqs. (7) are zero. This average of the oscillation is a function of the known spacecraft parameters and the initial burn and coast times, which are in turn a function of the integer number of revolutions, m and n, according to Eqs. (4).

Because nonzero values of $\tilde{\theta}_{\text{av}}$ reduce the final magnitude of the ΔV due to components of the thrust being perpendicular to the desired direction, ΔV is maximized by minimizing $\tilde{\theta}_{\text{av}}$. This task is accomplished by varying m and n (the number of revolutions during the burn and coast phases) and evaluating Eq. (10). The integral in Eq. (10) is performed only over the intervals when the thruster is on because $\tilde{\theta}$ deviations during the coast phase do not contribute to a loss of ΔV.

The solution of the improved two-burn scheme parameters (m and n) is dependent only on the spacecraft inertias, spin rate, and total burn time, all of which are known to reasonable precision. The moment M_x in Eqs. (5) can be factored out, so that the solution for m and n does not depend on knowledge of the direction or magnitude of the transverse torque, which is generally not known. The direction of the moment is arbitrary because the locations of $\hat{\boldsymbol{b}}_1$ and $\hat{\boldsymbol{b}}_2$ are arbitrary. The magnitude of the moment will only affect the relative benefit of the improved two-burn scheme over the two-burn and continuous thrust maneuvers; it does not effect the optimal burn and coast times.

IV. Results

The numerical example used to demonstrate the potential effectiveness of the improved two-burn scheme is based on a spacecraft with inertias

$$I_x = 5047\,\text{kg}\cdot\text{m}^2, \qquad I_z = 4627\,\text{kg}\cdot\text{m}^2 \tag{11}$$

This example was deliberately chosen to highlight the difference between the two-burn scheme and the improved two-burn scheme. Some inertias result in nearly insignificant differences between the two maneuvers.

The spacecraft for this example has a 400-N thruster with perfect alignment in the $\hat{\boldsymbol{b}}_3$ direction, but a 7.5-mm center-of-mass offset, which causes a 3-Nm body-fixed torque. The mass of the vehicle is 2000 kg, and the spin rate is 1.76 rpm. The total duration of the thruster firing is 300 s for a nominal ΔV of 60 m/s.

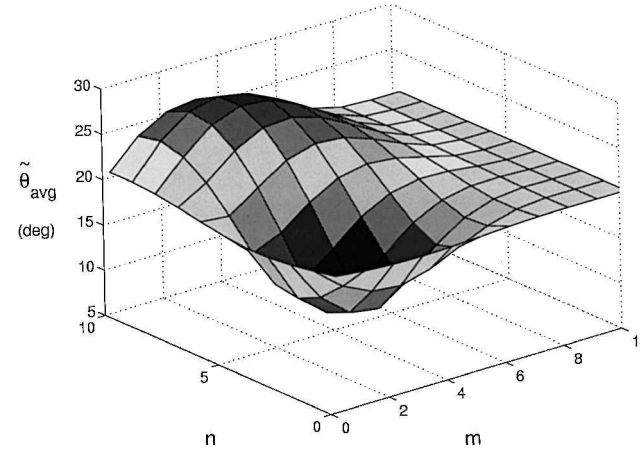

Fig. 6 Finding the optimal burn and coast times, m and n, for improved two-burn scheme.

To determine the optimal burn and coast times for the improved two-burn scheme, we vary m and n and numerically integrate to get the mean offset angle $\tilde{\theta}_{\text{av}}$ in Eq. (10). (Whereas the expression for $\tilde{\theta}$ is analytic, it is not integrable in closed form.) The results are shown in Fig. 6. The value of the angular deviation is nearly the same for all cases with $m \geq 8$. For our case of a spin rate of 1.76 rpm, the time of one full revolution is 34 s. Therefore, an m value of 8 yields an initial burn (before coast) of 272 s, which is nearly the entire duration of the 300-s burn. The case of $m = n = 0$ provides the original two-burn approach. Interestingly, the average offset (and, thus, the ΔV) is fairly insensitive to the initial burn, m, if the coast phase contains no extra revolutions ($n = 0$).

The optimal two-burn maneuver is found by examining Fig. 6 for the minimum $\tilde{\theta}_{\text{av}}$. This point is at $m = 2$ and $n = 3$, where the average angular displacement of the thrust axis is roughly half of the original two-burn scheme. Therefore, the optimal initial burn time lasts for two full revolutions plus an additional 60 deg, and the coast phase is three revolutions plus 60 deg. By our hypothesis, this maneuver should yield the largest ΔV. Figure 6 can also be used to evaluate suboptimal maneuvers in the event that constraints (such as total maneuver duration) do not permit the maximum ΔV maneuver.

Numerical simulation of the spacecraft attitude and translation dynamics is used to determine the exact ΔV resulting from the different maneuver types. The rotational and translational equations of motion for an axisymmetric rigid body are

$$\dot{\theta}_1 = (\omega_1 \cos\theta_3 - \omega_2 \sin\theta_3)/\cos\theta_2, \qquad \dot{\theta}_2 = \omega_1 \sin\theta_3 + \omega_2 \cos\theta_3$$

$$\dot{\theta}_3 = (-\omega_1 \cos\theta_3 + \omega_2 \sin\theta_3)\tan\theta_2 + \omega_3$$

$$\dot{\omega}_1 = -\alpha\omega_2 + M_x/I_x, \qquad \dot{\omega}_2 = \alpha\omega_1, \qquad \dot{\omega}_3 = 0$$

$$[v_X \quad v_Y \quad v_Z]^T = A[0 \quad 0 \quad f_z/m]^T \tag{12}$$

where ω_i is the angular velocity about the $\hat{\boldsymbol{b}}_i$ body axis, α is defined in Eq. (6), f_z is the thruster force along the thrust axis, A is the transformation matrix from the body to inertial frame, and v_X, v_Y, and v_Z are the components of velocity along the inertial coordinate axes. The kinematic equations for translation are not integrated because we are only concerned with the maneuver ΔV that is obtained by subtracting the velocity of the spacecraft at the beginning and end of the simulation. These first-order differential equations were integrated using a sixth-order Runge–Kutta algorithm with variable step size and a tolerance of 1×10^{-16}.

The results of the simulation for the continuous thrusting, two-burn scheme and the improved two-burn scheme are given in Table 1 and plotted in Figs. 7–10. Figures 7, 9, and 10 show the projection of the thrust axis of the spacecraft, $\hat{\boldsymbol{b}}_3$ onto the inertial $\hat{\boldsymbol{X}}$–$\hat{\boldsymbol{Y}}$ plane (Fig. 5). The axis is unit length, so that projections are fractions of unity. For nominal thrusting, this projection would be a point at the origin because the $\hat{\boldsymbol{b}}_3$ axis is aligned with $\hat{\boldsymbol{Z}}$. The time history of

Table 1 Performance of different maneuver types

Type	$\tilde{\theta}_{av}$, deg	Pointing error, deg	ΔV, m/s	% of nominal
No offset (theoretical maximum)	0	0	60	100
Improved two-burn scheme	8.93	0.52	59.12	98.53
Two-burn scheme	18.22	0.37	56.87	94.79
Continuous thrust	18.66	1.40	56.83	94.72

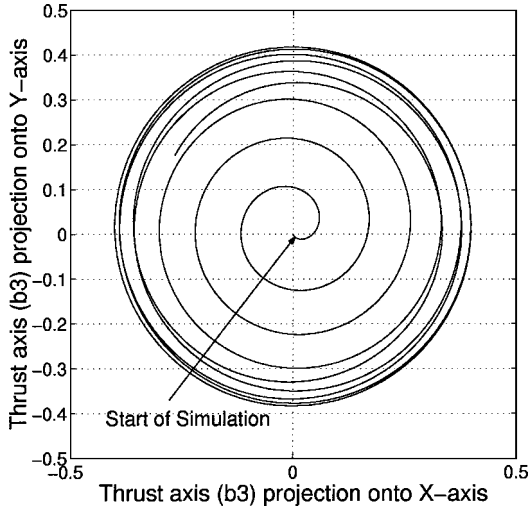

Fig. 7 Motion of the thrust axis, continuous thrust.

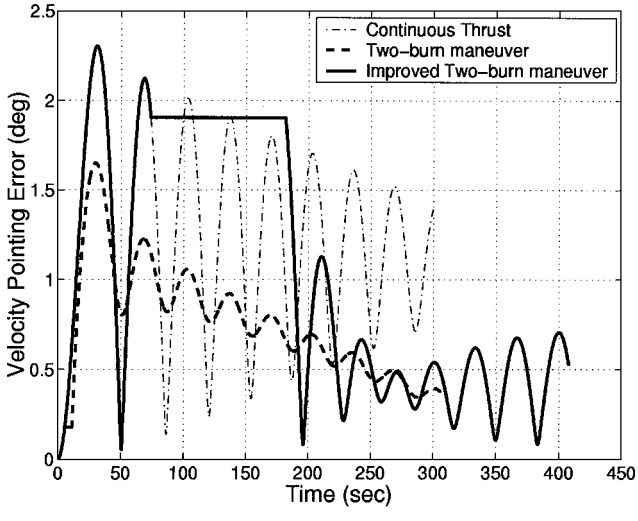

Fig. 8 Pointing error for three maneuver types.

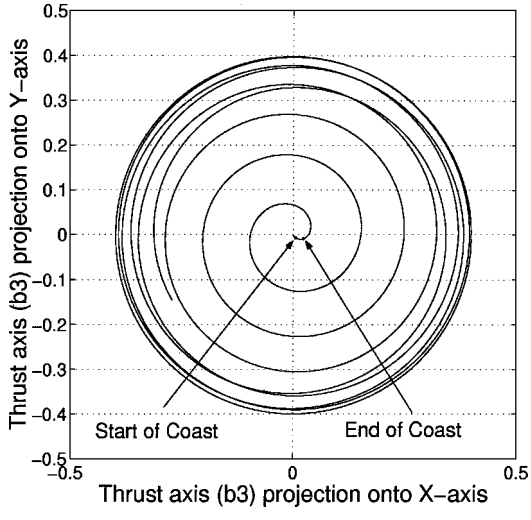

Fig. 9 Motion of thrust axis, two-burn scheme.

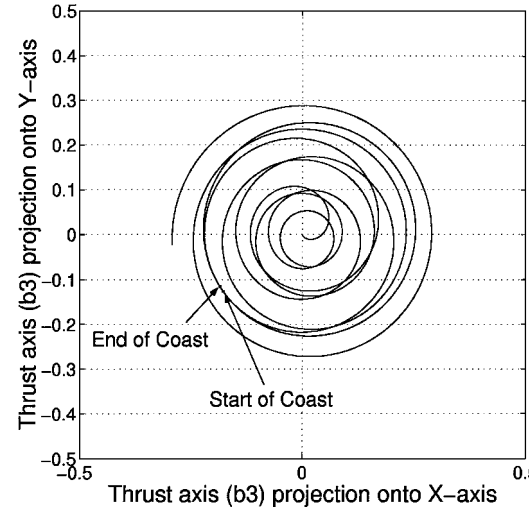

Fig. 10 Motion of thrust axis, improved two-burn scheme.

the angle between the velocity vector and the desired $\hat{Z}$ direction is plotted in Fig. 8 for each of the three cases.

Without any coast phase, the thrust axis follows the epicycle in Fig. 7. This precession of the thrust axis, which has an average angular displacement of 18.66 deg from the inertial Z axis, causes a significant loss in the final ΔV. The final ΔV of 56.83 m/s is roughly equal to the nominal value of 60 m/s times the cosine of the 18.66-deg displacement. This ΔV represents a loss of 5.28% compared to a perfectly aligned thruster (Table 1). The angle between the velocity vector and the desired $\hat{Z}$ direction for this case is the dashed line in Fig. 8. The pointing error oscillates due to the thrust axis precession, and it is asymptotically approaching 1.1 deg (0.019 rad). This is due to a bias in the precession (ρ in Fig. 3) and is accurately predicted by Eq. (2). This steady-state pointing error is also evidenced in Fig. 7 as a bias of the motion of the thrust axis in the positive $\hat{Y}$ direction. The steady-state pointing error is quite small compared to the oscillation of the thrust axis because this simulated case has been chosen to highlight the differences between the original and the improved two-burn schemes.

Performing the two-burn scheme does little to reduce the magnitude of deviation of the thrust axis from the desired $\hat{Z}$ direction; thus, Fig. 9 is similar to the continuous case. As a result, the final ΔV magnitude is nearly identical to the earlier continuous thrust case. The coast phase, however, is successful in removing the bias of the oscillation and so Fig. 9 does not have the 0.019-rad offset present in the Fig. 7. As a result, the pointing error is reduced to 0.39 deg, as shown in Fig. 8, and eventually approaches zero for very long burns.

The new maneuver, shown in Fig. 10, significantly reduces the deviation of the thrust axis from the Z axis. This reduction in coning angle yields a final ΔV of 59.12 m/s, which is an increase of about 2.3 m/s from the earlier two cases. However, the pointing error in Fig. 8 is slightly increased. The increasing amplitude oscillations in the pointing error toward the end of the maneuver do not increase, but instead approach a steady-state error of about 0.5 deg (after several more minutes). The steady-state pointing error is not eliminated for this case because the expressions that govern the burn and coast times are based on a linearized set of equations of motion that explicitly assume small angular deviations from the desired $\hat{Z}$ direction. The angle between the thrust axis and the $\hat{Z}$ axis for this improved two-burn example is 12.6 deg at the start and end of the coast phase (the critical junctures in the maneuver). For cases in which these angles are small (e.g., 0.5 and 1.5 deg at the start and end of the coast for the two-burn maneuver in Fig. 9), the improved two-burn maneuver does result in an oscillation centered on the origin with a zero steady-state pointing error.

An alternative to the discussed procedure would be a nonlinear programming algorithm used in conjunction with numerical simulation to optimize the burn and coast time to maximize the ΔV magnitude while eliminating the secular pointing error. The method

used here has the primary advantage of being much faster to compute because it does not require any simulation. Our method is also extremely robust because it is not iterative. Its primary weakness is the small angle assumption mentioned in the preceding paragraph. However, because the aim of spin stabilization is to keep the thrust axis deviations within a reasonable magnitude, the linear approximation should not pose a significant limitation. Of course, the analytic formulation developed here could also be used to provide initial guesses for more precise numerical searches.

To help validate the conjecture that minimizing $\tilde{\theta}_{\text{av}}$ will maximize ΔV, all of the cases from Fig. 6 ($0 \leq m \leq 10$ and $0 \leq n \leq 10$) have been simulated. The resulting ΔV is plotted against the semi-analytic $\tilde{\theta}_{\text{av}}$ in Fig. 11. The plot does display the trend that higher ΔV occur when the amplitude of the precession is small, but the plot is not perfectly monotonic. The nonsmooth nature of the plot

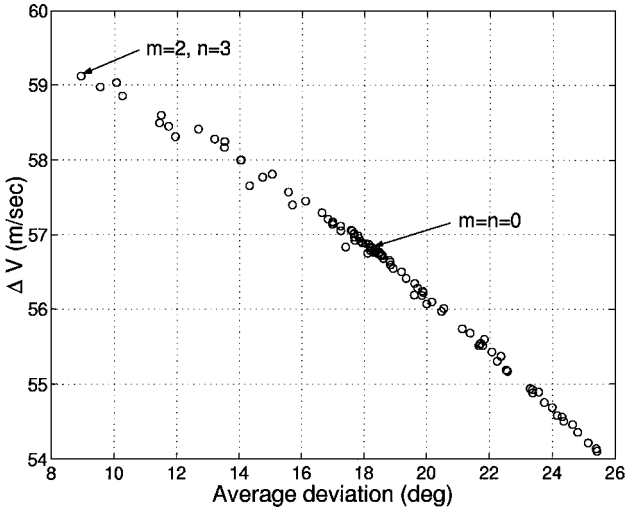

Fig. 11 Correlation between average angular deviation and magnitude of total ΔV.

is probably due to the small angle assumption. (Note that the error in this assumption does not increase smoothly with increasing $\tilde{\theta}_{\text{av}}$ because this parameter is not correlated with the maximum amplitude encountered during the maneuver.) This may introduce some errors into the optimal burn and coast times, but the computational efficiency of this formulation (vs numerical optimization methods) is probably worth this small sacrifice in accuracy.

V. Conclusions

Consideration of the attitude dynamics of the thrust axis of a spin-stabilized spacecraft reveals multiple solutions for burn and coast times that significantly reduce or eliminate the pointing error of a thrusting spacecraft. The improved two-burn scheme optimizes over the set of these maneuvers to minimize the magnitude of the thrust axis precession and, thereby, maximize the final ΔV. Analytic solutions for the time history of the oscillation of the thrust axis are used to find the optimal burn and coast times. For the case shown, the new maneuver scheme significantly improves the percentage of ΔV acquired compared to both continuous thrust and the previously developed two-burn maneuver. This solution depends only on known spacecraft properties and does not require explicit a priori knowledge of the transverse moment. This new maneuver may be used to increase accuracy and to decrease fuel expenditure for orbital injection and large orbit correction maneuvers.

References

[1] Longuski, J. M., Kia, T., and Breckenridge, W. G., "Annihilation of Angular Momentum Bias During Thrusting and Spinning Maneuvers," *Journal of the Astronautical Sciences*, Vol. 37, No. 4, 1989, pp. 433–450.

[2] Beck, R. A., and Longuski, J. M., "Annihilation of Transverse Velocity Bias During Spinning-Up Maneuvers," *Journal of Guidance, Control, and Dynamics*, Vol. 20, No. 3, 1997, pp. 416–421.

[3] Javorsek, D., and Longuski, J. M., "Velocity Pointing Errors Associated with Spinning Thrusting Spacecraft," American Astronautical Society, AAS Paper 99-452, Aug. 1999.

[4] Wie, B., *Space Vehicle Dynamics and Control*, AIAA, Reston, VA, 1998, pp. 352–354.